

# On-Surface Porphyrin Transmetalation by Pb/Cu Redox Exchange

Jan Herritsch, Stefan R. Kachel, Qitang Fan, Mark Hutter, Lukas Heuplick, Florian Münster,  
J. Michael Gottfried\*

*Department of Chemistry, Philipps University of Marburg, Hans-Meerwein-Straße 4, 35032 Marburg,  
Germany, michael.gottfried@chemie.uni-marburg.de*

## Abstract

Metal complexes at surfaces and interfaces play an important role in many areas of modern technology, including catalysis, sensors, and organic electronics. An important aspect of these interfaces is the possible exchange of the metal center, because this reaction can drastically alter the properties of the metal complex and thus of the interface. Here, we demonstrate that such metal exchange reactions are indeed possible and can proceed already at moderate temperatures even in the absence of solvents. Specifically, we studied the redox transmetalation of a monolayer of lead(II)-tetraphenylporphyrin (PbTPP) with copper from a Cu(111) surface under ultrahigh-vacuum (UHV) conditions using multiple surface-sensitive techniques. Temperature dependent X-ray photoelectron spectroscopy (XPS) reveals that the Pb/Cu exchange starts already below 380 K and is complete at 600 K. The identity of the reaction product, CuTPP, is confirmed by mass spectrometric detection in a temperature-programmed reaction (TPR) experiment. Scanning tunneling microscopy (STM) sheds light on the adsorbate structure of PbTPP at 300 K and uncovers the structural changes accompanying the transmetalation and side-reactions of the phenyl substituents. Moreover, individual free Pb atoms are observed as a product of the metal exchange. Our study suggests that surfaces functionalized with metal complexes may consist of other species than intended under operation conditions, which often involve elevated temperatures.

## Introduction

Tetrapyrrole ligands such as porphyrins and phthalocyanines provide a defined coordination environment for metal cations and are widely used in catalysis<sup>1-3</sup>, in sensor technology<sup>4</sup> but also as components in molecular electronics<sup>5-6</sup>. Typically, the chemical and optoelectronic properties of the complexes are largely determined by the incorporated cation. Hence, their reactivity is given by the electronic structure of the central atom, i.e., by the number of occupied and unoccupied metal states and their energy level as well as their spatial distribution. By varying the central atom or its redox state, the valence electronic structure and thus the reactivity can be specifically altered.

A reaction by which the incorporated central atom of a porphyrin or phthalocyanine complex is exchanged by another element can drastically change the properties of the complex. Such a reaction, also referred to as transmetalation, is well-known from solution chemistry<sup>7-8</sup> and was also investigated at the solid/liquid interface.<sup>9</sup> In the presence of solvents, which stabilize ionic states, the reaction is an ion exchange, i.e., the oxidation state of the metal ions remains unchanged during the transmetalation. In contrast, transmetalation at the solid/solid (e.g., complex/metal) interface is a redox reaction, in which the leaving metal ion is reduced, while the entering metal atom is oxidized. It has been claimed that such redox transmetalation reactions of tetrapyrrole complexes occur on metal surfaces with surface adatoms<sup>10-11</sup> or with other metal atoms.<sup>12</sup> In these reports, the transmetalation was deduced from the apparent reduction of the leaving central ion,  $M(II) \rightarrow M(0)$ , as observed by X-ray photoelectron spectroscopy (XPS), near-edge X-ray absorption fine-structure (NEXAFS) spectroscopy. However, this reduction does not provide sufficient evidence for transmetalation: First, the observed shifts towards lower binding energies can also be caused by charge transfer from the metal surface to the intact complex, as has frequently been observed.<sup>13-18</sup> Second, to confirm transmetalation, it still needs to be shown that another metal replaces the original metal center. The incomplete conversion in some of the proposed metal exchange reactions<sup>10</sup> points towards electron transfer rather than transmetalation. For example, for the claimed exchange reaction between a nickel(II) porphyrin and the underlying Cu(111) surface, the only partial transformation (60-70%) of Ni(II) to Ni(0) was explained by a chemical equilibrium between Ni(II) porphyrin and Cu(II) porphyrin.<sup>10</sup> However, considering the almost infinite excess of Cu in this experiment, an equilibrium should be completely on the side of the product, Cu(II) porphyrin. In contrast, the simultaneous presence of M(II) and M(0) oxidation states is in line with electron transfer, which is highly dependent on the adsorption site, resulting in monolayer phases of intact metalloporphyrins with mixed oxidation states of the metal centers.<sup>14,19</sup> Therefore, previous work has not resolved the question whether tetrapyrrole complexes can undergo metal exchange in the absence of solvents. Below, we will present the first unambiguous mass spectrometric evidence that such metal exchange redox reactions are indeed possible.

Compared to the extensively studied transition metal complexes, post-transition metal tetrapyrroles received less attention in surface and interface science.<sup>14</sup> Especially lead(II) complexes have rarely been

investigated<sup>20-23</sup> and there are no related studies of Pb(II) porphyrins. Due to the large ionic radius of Pb(II), these complexes adopt a non-planar structure with an out-of-plane bound metal center.<sup>24</sup> According to crystal structure data, the Pb ion is located about 1.2 Å above the center of the N<sub>4</sub> plane forming a square pyramid.<sup>24-26</sup> As a result, Pb tetrapyrroles differ considerably from their transition metal analogues with an N<sub>4</sub> in-plane coordination of the central atom (Figure 1). The combination of the large ionic radius and the highly undercoordinated Pb atom enables a diverse coordination chemistry of Pb(II) tetrapyrroles.<sup>27-28</sup> Furthermore, the complexes are known to engage in metal-exchange reactions in solution chemistry.<sup>27, 29-30</sup> In the adsorbed state, the out-of-plane bound metal center can either point towards the surfaces (metal-down conformer) or away from the surface (metal-up conformer). For Pb(II) phthalocyanine (PbPc) on Ag(111), both conformers could be distinguished by STM.<sup>23</sup> Moreover, it was claimed that PbPc undergoes detachment of the central atom by interactions with Pt(111)<sup>21</sup> and Ag(111)<sup>22</sup> metal substrates as well as InSb(100) and InAs(100) III-V semiconductors.<sup>20</sup> This reaction was deduced from the apparent reduction of Pb(II), but the products remained unidentified, leaving the question of transmetalation again unresolved.

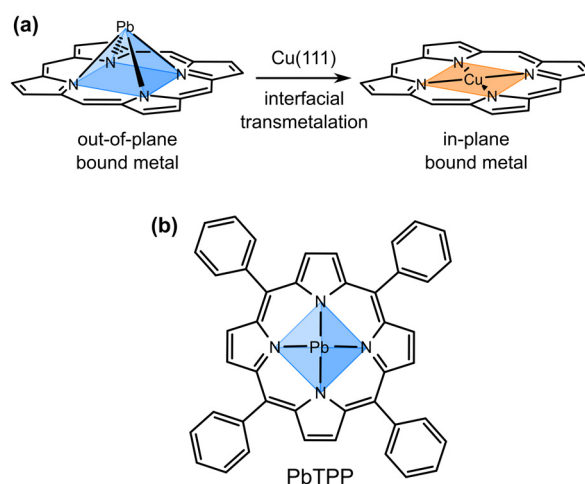


**Figure 1.** (a) Transmetalation of a Pb(II) porphyrin by reaction with a Cu(111) surface:  $\text{PbTPP} + \text{Cu} \rightarrow \text{CuTPP} + \text{Pb}$ . The coordination environment of the out-of-plane bound and the in-plane bound metal center is colored in blue and orange, respectively. (b) Molecular structure of Pb(II) 5,10,15,20-tetraphenylporphyrin (PbTPP).

Here, we show that Pb(II)-tetraphenylporphyrin (PbTPP, Figure 1b) engages in a redox transmetalation reaction with Cu atoms from a Cu(111) surface, resulting in the formation of CuTPP. The conversion of PbTPP to CuTPP is unambiguously confirmed by mass spectrometry. By temperature-dependent reaction monitoring with XPS, we show that the exchange reaction starts already at moderately elevated temperatures between 350 K and 380 K. With STM, the structural changes related to the reaction progress are observed in the single-molecule level and side reactions of the porphyrin ligand are clarified.

## Experimental Methods

All experiments were performed in ultrahigh vacuum (UHV) with a base pressure in the range of  $10^{-10}$  mbar. PbTPP (purity > 95%) was purchased from Por-Lab, Porphyrin Laboratories GmbH. The Cu(111) single crystals (purity > 99.9999%, roughness < 0.03  $\mu\text{m}$ , orientation accuracy < 0.1°, MaTecK/Germany) were cleaned by repeated cycles of  $\text{Ar}^+$  ion bombardments (0.5 keV) followed by annealing (> 800 K). Surface cleanliness was confirmed by XPS prior to the XPS and STM experiments. XPS and STM were performed in a two-chamber UHV setup using a monochromatized Al K $\alpha$  X-ray source (1486.7 eV) and a SPECS Phoibos 150 electron energy analyzer equipped with an MCD-9 multi channeltron detector as well as a SPECS Aarhus 150 STM. The samples were prepared in-situ by vapor deposition of PbTPP (610 K) onto the clean Cu(111) surface held at room temperature. The purity of the deposited PbTPP films, especially the absence of the free-base 2HTPP, was confirmed by XPS measurements (Figure S1 in the Supporting Information). The flux was monitored at the sample position using a quartz crystal microbalance. A coverage of 1 ML refers here to the number of adsorbed molecules in a closely packed monolayer. All coverages were determined by the C 1s XPS intensities. For STM, the sample was cooled to about 100 K with  $\text{l-N}_2$  and images were obtained in constant current mode. For a background correction of the XPS spectra in the N 1s and Pb 4f regions, spectra of the pristine Cu(111) surface were used. The background spectra were interpolated by a smoothing spline and afterwards the spline function was subtracted from the measured spectra. TPR experiments were carried out using a HIDEN EPIC 1000 quadrupole mass spectrometer mounted inside a differentially pumped cryo shroud cooled to 90 K with  $\text{l-N}_2$ . The used setup<sup>31-32</sup> enables the detection of the intact molecule ions of CuTPP ( $m/z = 675$ ) and PbTPP ( $m/z = 820$ ). For TPR, the substrate was held at 100 K during deposition of PbTPP. The prepared sample was placed in front of the orifice (8 mm diameter) of the cryo shroud and the crystal was heated resistively via tungsten wires with a constant rate of 1 K/s. Temperatures were measured using a calibrated Type K thermocouple mounted inside the sample.

## Results and Discussion

*Temperature-dependent XPS.* The temperature-dependent transformations of a PbTPP monolayer on a Cu(111) surface were monitored by XPS between 300 K and 600 K. For three selected temperatures, the Pb 4f XP spectra are shown in Figure 2a, while a detailed temperature series with Pb 4f, C 1s, and N 1s XPS data is presented in the supporting information (SI), Figure S2. For comparison with the monolayer XPS data, Figure 2b shows the Pb 4f spectrum of a PbTPP multilayer film. The corresponding C 1s and N 1s spectra are shown in Figure S1 in the SI. In the PbTPP multilayer spectrum, the spin-orbit components are well separated at binding energies (BEs) of 138.5 eV and 143.4 eV for the Pb 4f<sub>7/2</sub> and Pb 4f<sub>5/2</sub> signal, respectively, consistent with spectra of other Pb(II) tetrapyrrole complexes.<sup>21-22, 33-34</sup> Relative to the multilayer peak position, only a slight shift towards lower BEs (138.3 eV and 143.2 eV) is observed for the monolayer at 300 K (Figure 2a). However, after annealing to higher temperatures, a

second doublet appears at lower BEs of 136.6 eV and 141.5 eV. This doublet is assigned to a reduced species, possibly Pb(0), which may indicate formation of Pb(0) atoms as a product of the transmetalation. Alternatively, possible temperature-driven structural transformations of the monolayer film the lower BE may lead to increased electron transfer from the surface to the Pb center of the intact complex. Therefore, the chemical shift of the Pb 4f signal is not a sufficient evidence for a detachment of the Pb atom from the complex as a prerequisite for transmetalation.

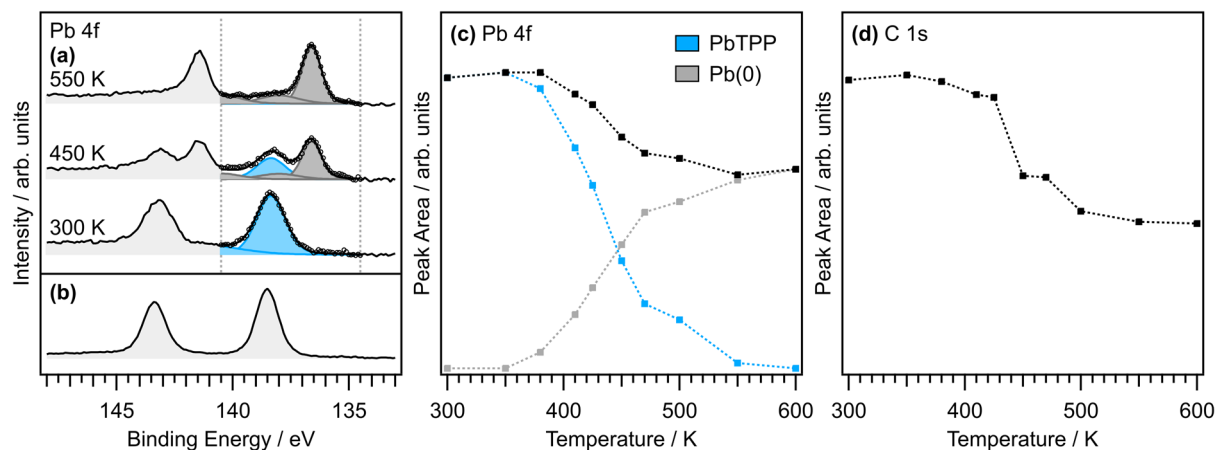


**Figure 2.** Pb 4f XP spectra of (a) an as-deposited PbTPP monolayer on Cu(111) at 300 K and after annealing to the indicated temperatures (450 K, 550 K) for 3 min. The Pb 4f<sub>7/2</sub> region between 134.5 eV and 140.5 eV is described by a fit of the Pb(II) (colored in blue) and the Pb(0) (colored in gray) moieties. Here, the black line is the sum of both components while open circles represent the experimental data. The monolayer spectra can be compared with (b) a PbTPP multilayer (thickness 4.0 nm). (c) In a more detailed temperature series, Pb 4f signal areas and the sum of both components area are given for different temperatures as well as (d) the concurrent progression of the C 1s peak area. Corresponding spectra can be found in the SI (Figure S2).

For quantification of the temperature evolution, the Pb 4f<sub>7/2</sub> regions in Figure 2a and Figure S2c were analyzed through a thorough fitting procedure. In Figure 2a, comparison of the areas of the Pb(II) signal (blue fit function) with those of the Pb(0) signal (grey fit function) shows that about 55% of the Pb atoms have already been reduced after annealing to 450 K. Further heating to 550 K leads to almost full conversion. Figure 2c shows the areas of the Pb(II) and the Pb(0) components of the more detailed temperature series presented in Figure S2. As can be seen, the transformation from Pb(II) to Pb(0) starts already between 350 K and 380 K and is complete at 600 K. Moreover, a decrease in the overall Pb 4f intensity above 425 K is observed.

The corresponding C 1s signals (Figure 2d) also show a temperature-dependent decrease in intensity, which is even more pronounced and accompanied by a change of the peak shape (see Figure S2b). The decreasing intensities indicate partial desorption of the monolayer, while changes in the C 1s peak shape

suggest that the remaining complexes undergo reactions at the porphyrin ligand. The STM data presented further below confirm intermolecular cyclodehydrogenation reactions of the peripheral phenyl substituents at higher temperatures. This side reaction is a commonly observed behavior of the TPP ligand and results in a planar structure of the molecule, as has frequently been described in the literature.<sup>35-43</sup> With this planar structure, it is no longer possible for attractive  $\pi$ -stacking interactions between the phenyl rings to keep the individual molecules densely-packed together, resulting in increased lateral repulsion. It is therefore proposed that the flattening of the residual molecules facilitates the partial desorption of the monolayer above 425 K. It is important to note that the relative decrease is larger for C 1s than for Pb 4f (compare Figure 2c and 2d), which means that not only PbTPP desorbs, but also some additional carbon-containing species. In the following, we use mass spectrometry to show that this additional desorbing species is CuTPP as the product of the transmetalation reaction.

*TPR measurements.* According to XPS, the Pb(0) species appears already around 380 K, i.e., well below the onset of partial desorption, which starts above 425 K. Therefore, if the Pb(0) species stems from transmetalation, CuTPP as the other reaction product should be among the desorbing species, besides PbTPP. It is important to note that desorption occurs only in the range between a full monolayer and  $\sim 0.5$  ML (cf. Figure 2d). Therefore, the TPR measurements were performed on a partially pre-covered surface obtained by partial thermal desorption of a full PbTPP monolayer. In successive TPR cycles, layers of PbTPP with increasing thickness were deposited onto the sample, which was subsequently annealed with a constant heating rate (1 K/s) to 650 K. During annealing, the desorption of PbTPP ( $m/z = 820$ ) and CuTPP ( $m/z = 675$ ) was recorded by mass spectrometry. Using the pre-covered surface, we succeeded to desorb the molecules intact (i.e., without loss of hydrogen atoms), enabling the detection of the molecule ions with the expected masses.

Figure 3 shows TPR traces for increasing amounts of PbTPP deposited on the pre-covered Cu(111) surface. For the lowest coverage (Figure 3a), only the desorption of CuTPP in the range from 510 K to 605 K is observed, indicating complete transmetalation of PbTPP. After increasing the amount of deposited PbTPP (Figure 3b), the CuTPP signal saturates and small amounts of PbTPP desorb between 490 K and 555 K. The CuTPP peak gets slightly broadened and the peak maximum shifts to lower temperatures, caused by the increased intermolecular repulsion at higher coverages. For even higher initial dosages (Figure 3c), only the PbTPP desorption peak increases and gets broadened, while the amount of desorbing CuTPP remains constant. Once saturation of the CuTPP peak is reached, no changes in peak form or desorption maximum are observed anymore (Figure 3c,d). At the highest coverage (Figure 3d), the bilayer peak (485 K) as well as a small multilayer shoulder (475 K) are observed, confirming that an excess of PbTPP has been deposited. Note that no transmetalation reaction is found in the multilayer. Formation of CuTPP by metalation of a 2HTPP contaminant can be excluded, based on XPS studies of the deposited pristine PbTPP films (see Figure S1 in the SI).

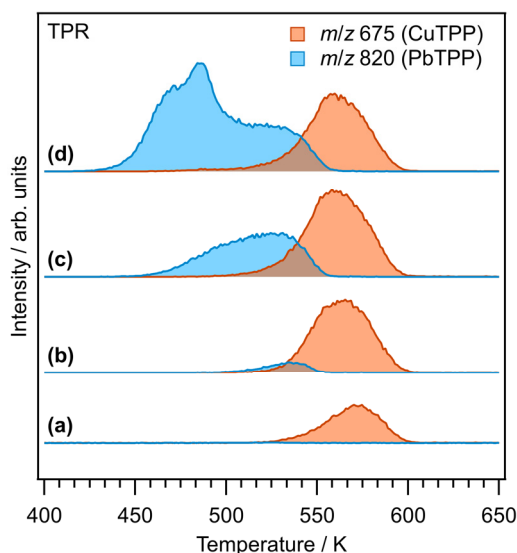


**Figure 3.** Traces of sequential TPR experiments with the recorded mass-to-charge ratios  $m/z = 675$  (CuTPP) and  $m/z = 820$  (PbTPP). PbTPP was deposited onto pre-covered Cu(111) with increasing dosages of PbTPP from (a) to (d). The signal contributions below  $\sim 500$  K in (c) and (d) belong to multilayer desorption. The heating rate was 1 K/s in all experiments.

*STM measurements.* Having confirmed the transmetalation reaction by identifying the product CuTPP by mass spectrometry, we now want to obtain insight into the adsorbate structure of PbTPP on Cu(111) and characterize the reaction products that remain on the surface. For this aim, submonolayers with two different coverages (0.25 ML and 0.40 ML) were investigated by STM, providing details on structural changes of the individual molecules upon transmetalation and the side-reactions of the peripheral phenyl substituents. In a submonolayer with low coverage (0.25 ML), the molecules are well separated and do not aggregate into islands. The individual PbTPP molecules appear all in the same rectangular shape with a characteristic protrusion in the center (Figures 4a and 5a). Porphyrin complexes with an out-of-plane bound metal sometimes adsorb in two distinguishable conformers, in which the central atom is located between the porphyrin and the underlying metal substrate (metal-down conformer) or above the ring (metal-up conformer).<sup>14, 23</sup> This is not the case here, since only one species is observed. The highly distorted shape suggests that the molecule interacts strongly with the surface and is chemisorbed. The molecular features observed in STM suggest an adsorbate structure as shown by the molecular formula in Figure 4a, right. Here, the molecule including the peripheral phenyl substituents adsorbs flat on the surface, except for two upright-standing pyrrole units. A similar adsorbate structure, which is referred to the inverted conformer in the literature,<sup>44-45</sup> has also been observed for the free ligand 2HTPP on Cu(111). Bending of the two upright-standing pyrrole units provides additional space for the incorporated Pb atom and explains the absence of a metal-down and metal-up conformer. Due to the increased Pb–N distance, it can be assumed that the metal-ligand bond is already weakened in this adsorbate structure. The proposed structure also explains why the molecules do not tend to form islands at low

coverage of 0.25 ML. Because the peripheral phenyl substituents lie flat on the surface, no attractive intermolecular  $\pi$  stacking or T-type interactions can be established. As a result, lateral repulsion between the adsorption-induced surface dipoles prevails. However, after increasing the coverage to 0.40 ML, the molecules also form islands (see Figure S3). In these island, they adopt a different conformation, in which the phenyl rings are tilted relative to the surface plane and thus enable attractive T-type and  $\pi$  stacking interactions.<sup>14,46</sup> Note that the islands disappear after annealing the sample.

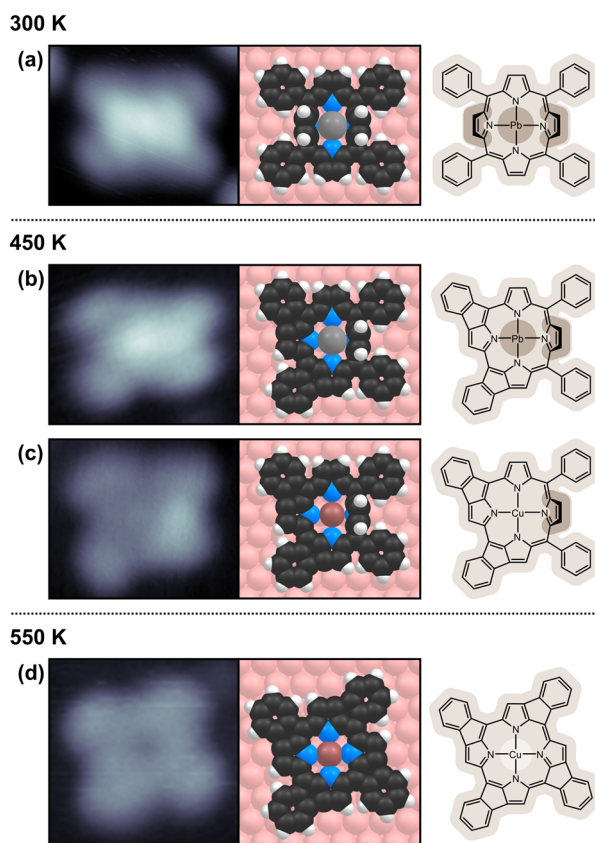


**Figure 4.** Left, STM images of individual molecules in a PbTPP submonolayer (0.25 ML) on Cu(111); center, proposed adsorbate structures; right, the corresponding molecular structure with shadings highlighting protruding parts. (a) PbTPP after deposition at 300 K, (b-c) selected partially reacted molecules after annealing to 450 K, and (c) product of the completed transmetalation and dehydrogenation after annealing to 550 K. Tunneling parameters: (a)  $U = -2.75$  V,  $I = -0.21$  nA; (b)  $U = -0.69$  V,  $I = -0.16$  nA; (c)  $U = -0.69$  V,  $I = -0.14$  nA; (d)  $U = -0.99$  V,  $I = -0.15$  nA.

Annealing the sample with 0.25 ML to 450 K causes structural changes of the molecule, which are attributed to the well-established step-wise cyclodehydrogenation of the peripheral phenyl substituents. In the course of this side reaction, which has extensively been investigated for the free ligand 2HTPP<sup>35-43</sup> and various TPP metal complexes<sup>42-43</sup>, the molecules become flattened. Besides these changes of the ligand structure, we also find that the centers of the molecules have different apparent heights, which indicates that some of the molecules have already completed the metal-exchange reaction and formed a



Cu complex, while others still contain the Pb center inside the macrocycle. For selected molecules, STM images including proposed molecular structures are shown in Figure 4b,c. In (b), a molecule with partial cyclodehydrogenation between the phenyl rings and the porphyrin macrocycle is shown. In the course of this reaction, one of the two upright standing pyrrole units becomes flat. Moreover, the bright protrusion in the center indicates that Pb(II) is still embedded inside the macrocycle. In contrast, (c) shows a molecule in which the substituents have reacted like in (b), but without the elevation in the center of the ring. Thus, this molecule has already lost the Pb(II) atom. Whether there is already a Cu(II) atom incorporated cannot be definitely concluded. However, the center of the macrocycle does not appear as a dark pore and it can be assumed that there is already Cu(II) inside. Further annealing to 550 K leads again to a change in the appearance of the individual molecules (Figure 4d). Most of the molecules are completely flat-lying on the surface without any bright features. This can be explained by the completion of the dehydrogenative side-reaction as well as the release of the bulky lead atom from the porphyrin macrocycle.

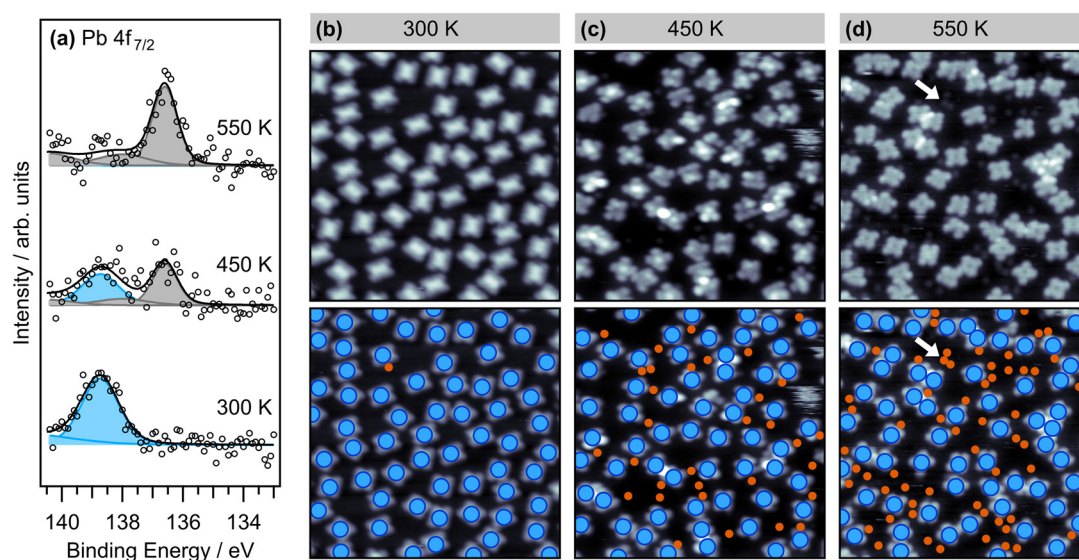


**Figure 5.** (a) Pb 4f spectra of a PbTPP submonolayer (0.25 ML) on Cu(111) at 300 K and after annealing to 450 K and 550 K as indicated. (b-c) STM images of the same samples. Each of the upper STM images shows an area of 20.0×20.0 nm<sup>2</sup>. The bottom STM images are the same as those above, but with overlaid blue circles representing the molecules and orange circles representing visible Pb(0) atoms. Tunneling parameters: (b)  $U = -2.75$  V,  $I = -0.13$  nA; (c)  $U = -0.69$  V,  $I = -0.16$  nA; (d)  $U = -0.97$  V,  $I = -0.23$  nA. Annealing temperatures and progress of the Pb → Cu exchange: (b) 300 K, XPS = 0%, STM = 2%; (c) 450 K, XPS = 47%, STM = 53%; (d) 550 K, XPS = 94%, STM = 95%.

Figure 5 shows larger-scale STM images of the 0.25 ML sample at three selected temperatures and compares them to the corresponding Pb 4f<sub>7/2</sub> spectra. These XP spectra (Figure 5a) show that annealing to 450 K and 550 K leads to the same degrees of Pb(II) → Pb(0) conversion as were found for the

monolayer (compare to Figure 2 and see the SI for more details). At 300 K (Figure 5b), PbTPP exclusively occurs in the adsorbate structure introduced in Figure 4a. Annealing to 450 K (Figure 5c) results in a distribution of various types of partially reacted molecules. About half of the observed molecules have no bright center and therefore no incorporated Pb(II). In addition, small features can be seen located between the individual molecules. Those only weakly protruding dots can be assigned to Pb(0) atoms formed as a side product of the transmetalation. While at 450 K only a few of these are observed, further annealing to 550 K (Figure 5d) leads to a substantial increase of the number of Pb(0) atoms. This is in a good agreement with the fact that most of the molecules are completely flat-lying on the surface without any bright features. Only a few protruding structures can be recognized, which imply that a very small minority of macrocycles might still contain a lead atom or upright-standing substituents. Thus, at 550 K, both the release of the bulky Pb atom from the porphyrin macrocycle and the dehydrogenative side-reactions are almost complete. The progress of the Pb  $\rightarrow$  Cu exchange can be derived by counting the molecules and the individual Pb(0) atoms in the STM images for each temperature step (see details in the SI). According to this analysis, after annealing to 450 K about 53% of the molecules have already reacted and increasing the temperature to 550 K leads to a corresponding value of 95%. This is in a good agreement with 47% and 94% obtained by XPS, respectively. In Figure 6, the STM and XPS data for the submonolayer Pb  $\rightarrow$  Cu exchange are compared to the XPS data for the monolayer case (cf. Figure 2). As can be seen, the agreement between the three data sets is very good, which also indicates that the transmetalation is largely independent from the coverage.

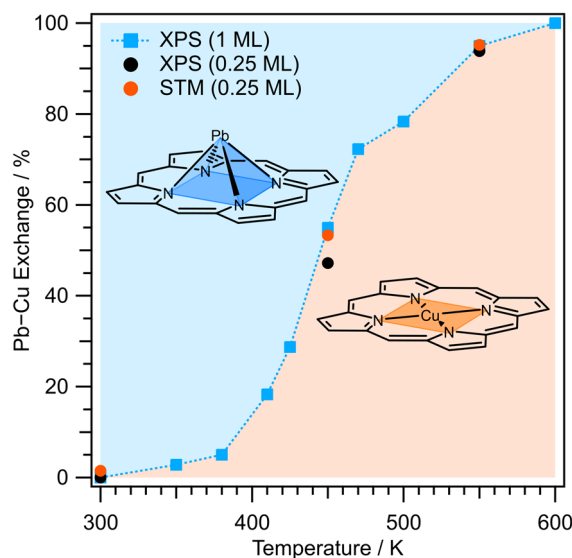


**Figure 6.** Temperature-dependence of the Pb  $\rightarrow$  Cu exchange reaction derived from XPS for 1 ML PbTPP (blue squares) and 0.25 ML PbTPP (black circles), compared to the corresponding STM values for 0.25 ML PbTPP (orange circles).

## Conclusion

Lead(II) tetraphenylporphyrin (PbTPP) undergoes transmetalation with copper atoms from a Cu(111) surface, resulting in the formation of copper(II) tetraphenylporphyrin (CuTPP) and Pb(0) atoms. This irreversible reaction starts above 350 K and is complete by 600 K, as was shown for monolayers and submonolayers by temperature-dependent XPS and STM measurements. Partial desorption of the reactants enabled the unambiguous identification of the product CuTPP by mass spectrometry in a TPR experiment. Unlike porphyrin transmetalation in solution or at the metal/solution interface, which proceeds via ion exchange, the on-surface transmetalation is a redox reaction involving reduction of released metal and oxidation of the entering metal. However, a reduction of the released metal is not a sufficient proof for transmetalation, because of the metal's oxidation state can also be reduced by electron transfer from the substrate to the intact complex. The temperature-dependent adsorbate structure was investigated in detail by STM. Intact PbTPP adopts a distorted structure with flat-lying phenyl substituents and two tilted pyrrole units. In this conformation, the ligand provides additional space inside the cavity to accommodate the large Pb(II) ion. As a result of this conformational adaptation, only one conformer occurs, instead of a mixed phase of metal-up and metal-down conformers. After annealing, the release of Pb is confirmed by the loss of the bright protrusion in the porphyrin center and the appearance of additional features on the surface attributed to the released Pb(0) atoms. In addition, structural changes of the ligand occur, which are related to cyclodehydrogenation at the periphery of the macrocycle. At 450 K, this side reaction leads to various partially reacted products, while further annealing to 550 K produces entirely flat-lying molecules with uniform height.

## Acknowledgements

Financial support by the Deutsche Forschungsgemeinschaft (DFG) through the SFB 1083 "Structure and Dynamics of Internal Interfaces" (223848855-SFB 1083) is gratefully acknowledged.

## Supporting Information

Additional multilayer XP spectra, a detailed monolayer temperature-dependent XP series as well as description of the island conformer and the temperature-dependent yield of the transmetalation.

## References

1. Zhang, W.; Lai, W.; Cao, R., Energy-Related Small Molecule Activation Reactions: Oxygen Reduction and Hydrogen and Oxygen Evolution Reactions Catalyzed by Porphyrin- and Corrole-Based Systems. *Chem. Rev.* **2016**, *117*, 3717-3797.
2. Barona-Castano, J. C.; Carmona-Vargas, C. C.; Brocksom, T. J.; Oliveira, K. T. d., Porphyrins as Catalysts in Scalable Organic Reactions. *Molecules* **2016**, *21*, 1-27.
3. Pereira, M. M.; Dias, L. D.; Calvete, M. J. F., Metalloporphyrins: Bioinspired Oxidation Catalysts. *ACS Catal.* **2018**, *8*, 10784-10808.
4. Paolesse, R.; Nardis, S.; Monti, D.; Stefanelli, M.; Natale, C. D., Porphyrinoids for Chemical Sensor Application. *Chem. Rev.* **2017**, *117*, 2517-2583.
5. Jurow, M.; Schuckman, A. E.; Batteas, J. D.; Drain, C. M., Porphyrins as molecular electronic components of functional devices. *Coord. Chem. Rev.* **2010**, *254*, 2297-2310.
6. Martynov, A. G.; Safonova, E. A.; Tsivadze, A. Y., Functional molecular switches involving tetrapyrrolic macrocycles. *Coord. Chem. Rev.* **2019**, *387*, 325-347.
7. Baker, H.; Hambright, P.; Wagner, L.; Ross, L., Metal Ion Interactions with Porphyrins. I. Exchange and Substitution Reactions. *Inorg. Chem.* **1973**, *12* (9), 2200-2202.
8. Berezin, D. B.; Shukhto, O. V.; Nikol'skaya, M. S.; Berezin, B. D., Some Peculiarities of Metal Exchange Reactions in Porphyrin and Phthalocyanine Complexes. *Russ. J. Coord. Chem.* **2005**, *31* (2), 95-100.
9. Franke, M.; Marchini, F.; Jux, N.; Steinrück, H.-P.; Lytken, O.; Williams, F. J., Zinc Porphyrin Metal-Center Exchange at the Solid-Liquid Interface. *Chem. Eur. J.* **2016**, *22*, 8520-8524.
10. Doyle, C. M.; Cunniffe, J. P.; Krasnikov, S. A.; Preobrajenski, A. B.; Li, Z.; Sergeeva, N. N.; Cafolla, M. O. S. A., Ni-Cu ion exchange observed for Ni(II)-Porphyrins on Cu(111). *Chem. Commun.* **2014**, *50*, 3447-3449.
11. Shen, K.; Narsu, B.; Ji, G.; Sun, H.; Hu, J.; Liang, Z.; Gao, X.; Li, H.; Li, Z.; Song, B.; Jiang, Z.; Huang, H.; Wells, J. W.; Song, F., On-surface manipulation of atom substitution between cobalt phthalocyanine and the Cu(111) substrate. *RSC Adv.* **2017**, *7*, 13827-13835.
12. Hötger, D.; Abufager, P.; Morchutt, C.; Alexa, P.; Grumelli, D.; Dreiser, J.; Stepanow, S.; Gambardella, P.; Busnengo, H. F.; Etzkorn, M.; Gutzler, R.; Kern, K., On-surface transmetalation of metalloporphyrins. *Nanoscale* **2018**, *10*, 21116.
13. Peisert, H.; Uihlein, J.; Petraki, F.; Chassé, T., Charge transfer between transition metal phthalocyanines and metal substrates: The role of the transition metal. *Journal of Electron Spectroscopy and Related Phenomena* **2015**, *204*, 49-60.
14. Gottfried, J. M., Surface Chemistry of Porphyrins and Phthalocyanines. *Surf. Sci. Rep.* **2015**, *70*, 259-379.
15. Hieringer, W.; Flechtner, K.; Kretschmann, A.; Seufert, K.; Auwärter, W.; Barth, J. V.; Görling, A.; Steinrück, H.-P.; Gottfried, J. M., The Surface Trans Effect: Influence of Axial Ligands on the Surface Chemical Bonds of Adsorbed Metalloporphyrins. *J. Am. Chem. Soc.* **2011**, *133* (16), 6206-6222.
16. Lukasczyk, T.; Flechtner, K.; Merte, L. R.; Jux, N.; Maier, F.; Gottfried, J. M.; Steinrück, H.-P., Interaction of Cobalt(II) Tetraarylporphyrins with a Ag(111) Surface Studied with Photoelectron Spectroscopy. *J. Phys. Chem. C* **2007**, *111*, 3090-3098.
17. Zamborlini, G.; Lüftner, D.; Feng, Z.; Kollmann, B.; Puschnig, P.; Dri, C.; Panighel, M.; Santo, G. D.; Goldoni, A.; Comelli, G.; Jugovac, M.; Feyer, V.; Schneider, C. M., Multi-orbital charge transfer at highly oriented organic/metal interfaces. *Nat. Commun.* **2017**, *8* (335), 1-8.
18. Zamborlini, G.; Jugovac, M.; Cossaro, A.; Verdini, A.; Floreano, L.; Lüftner, D.; Puschnig, P.; Feyer, V.; Schneider, C. M., On-surface nickel porphyrin mimics the reactive center of an enzyme cofactor. *Chem. Commun.* **2018**, *54*, 13423-13426.
19. Schmid, M.; Zirzmeier, J.; Steinrück, H. P.; Gottfried, J. M., Interfacial Interactions of Iron(II) Tetrapyrrole Complexes on Au(111). *J. Phys. Chem. C* **2011**, *115* (34), 17028-17035.

20. Giovanelli, L.; Papageorgiou, N.; Terzian, G.; Layet, J. M.; Mossoyan, J. C.; Mossoyan-Deneux, M.; Göthelid, M.; Lay, G. L., Electronic structure of self-assembled organic/inorganic semiconductor interfaces: lead phthalocyanine on InSb and InAs(100)-4x2/c(8x2). *J. Electron. Spect. Rel. Phen.* **2001**, *114-116*, 375-381.
21. Papageorgiou, N.; Mossoyan, J. C.; Mossoyan-Deneux, M.; Terzian, G.; Janin, E.; Göthelid, M.; Giovanelli, L.; Layet, J. M.; Lay, G. L., High resolution synchrotron radiation PES study of PbPc deposited on Pt(111). *Appl. Surf. Sci.* **2000**, *162-163*, 178-183.
22. Baran, J. D.; Larsson, J. A.; Woodley, R. A. J.; Cong, Y.; Moriarty, P. J.; Cafolla, A. A.; Schulte, K.; Dhanak, V. R., Theoretical and experimental comparison of SnPc, PbPc and CoPc adsorption on Ag(111). *Pys. Rev. B* **2010**, *81*, 075413.
23. Sperl, A.; Kröger, J.; Berndt, R., Electronic Superstructure of Lead Phthalocyanine on Lead Islands. *J. Phys. Chem. A* **2011**, *115*, 6973-6978.
24. T. Yamaki; Nobusada, K., Theoretical Study of Metal-Ligand Bonds in Pb(II) Porphyrins. *J. Phys. Chem. A* **2003**, *107*, 2351-2355.
25. Barkigia, K. M.; Fajer, J.; Adler, A. D.; Williams, G. J. B., Crystal and Molecular Structure of (5,10,15,20-Tetra-n-propylporphinato)lead(II): A "Roof" Porphyrin. *Inorg. Chem.* **1980**, *19*, 2057-2061.
26. Plater, M. J.; Aiken, S.; Gelbrich, T.; Hursthouse, M. B.; Bourhill, G., Structures of Pb(II) porphyrins: [5,10,15,20-tetrakis-triisopropylsilylethynylporphinato]lead(II) and [5,15-bis-(3,5-bis-tert-butylphenyl)-10,20-bis-triisopropylsilylethynylporphinato]lead(II). *Polyhedron* **2001**, *20*, 3219-3224.
27. Gac, S. L.; Boitrel, B., Structurally characterized bimetallic porphyrin complexes of Pb, Bi, Hg and Tl based on unusual coordination modes. *J. Porphyrins Phthalocyanines* **2016**, *20*, 1-17.
28. Lemon, C. M.; Brothers, P. J.; Boitrel, B., Porphyrin complexes of the period 6 main group and late transition metals. *Dalton Trans.* **2011**, *40*, 6591-6609.
29. Sayer, P.; Gouterman, M.; Connell, C. R., Metalloid Porphyrins and Phthalocyanines. *Acc. Chem. Res.* **1982**, *15*, 73-79.
30. Kawai, T.; Fujiyoshi, R.; Sawamura, S., Solvent extraction of zinc(II) and manganese(II) with 5,10,15,20-tetraphenyl-21H,23H-porphine (TPP) through the metal exchange reaction of lead(II)-TPP. *Solvent Extr. Res. Dev.* **2000**, *7*, 36-43.
31. Klein, B. P.; Heijden, N. J. v. d.; Kachel, S. R.; Franke, M.; Krug, C. K.; Greulich, K. K.; Ruppenthal, L.; Müller, P.; Rosenow, P.; Parhizkar, S.; Bocquet, F. C.; Schmid, M.; Hieringer, W.; Maurer, R. J.; Tonner, R.; Kumpf, C.; Swart, I.; Gottfried, J. M., Molecular Topology and the Surface Chemical Bond: Alternant Versus Nonalternant Aromatic Systems as Functional Structural Elements. *Phys. Rev. X* **2019**, *9*, 011030.
32. Kachel, S. R.; Klein, B. P.; Morbec, J. M.; Schöniger, M.; Hutter, M.; Schmid, M.; Kratzer, P.; Meyer, B.; Tonner, R.; Gottfried, J. M., Chemisorption and Physisorption at the Metal/Organic Interface: Bond Energies of Naphthalene and Azulene on Coinage Metal Surfaces. *J. Phys. Chem. C* **2020**, *124* (15), 8257-8268.
33. Rager, A.; Gompf, B.; Dürselen, L.; Mockert, H.; Schmeisser, D.; Göpel, W., Stability of Organic Thin Films on Inorganic Substrates: Prototype Studies Using Metal Phthalocyanines. *J. Mol. Electron.* **1989**, *5*, 227-238.
34. Ottaviano, L.; Lozzi, L.; Santucci, S.; Nardo, S. D.; Passacantando, M., PbPc growth on Si surfaces studied with XPS and various SPM techniques. *Surf. Sci.* **1997**, *392*, 52-61.
35. Xiao, Y.; Ditze, S.; Chen, M.; Buchner, F.; Stark, M.; Drost, M.; Steinrück, H.-P.; Gottfried, J. M.; Marbach, H., Temperature-Dependent Chemical and Structural Transformations from 2H-tetraphenylporphyrin to Copper(II)-Tetraphenylporphyrin on Cu(111). *J. Phys. Chem. C* **2012**, *116*, 12275-12282.
36. Di Santo, G.; Blankenburg, S.; Castellarin-Cudia, C.; Fanetti, M.; Borghetti, P.; Sangaletti, L.; Floreano, L.; Verdini, A.; Magnano, E.; Bondino, F.; Pignedoli, C. A.; Nguyen, M. T.; Gaspari, R.; Passerone, D.; Goldoni, A., Supramolecular Engineering through Temperature-Induced Chemical

- Modification of 2H-Tetraphenylporphyrin on Ag(111): Flat Phenyl Conformation and Possible Dehydrogenation Reactions. *Chem. Eur. J.* **2011**, *17* (51), 14354-14359.
37. Di Santo, G.; Castellarin-Cudia, C.; Fanetti, M.; Taleatu, B.; Borghetti, P.; Sangaletti, L.; Floreano, L.; Magnano, E.; Bondino, F.; Goldoni, A., Conformational Adaptation and Electronic Structure of 2H-Tetraphenylporphyrin on Ag(111) during Fe Metalation. *J. Phys. Chem. C* **2011**, *115* (10), 4155-4162.
  38. Di Santo, G.; Sfiligoj, C.; Castellarin-Cudia, C.; Verdini, A.; Cossaro, A.; Morgante, A.; Floreano, L.; Goldoni, A., Changes of the Molecule-Substrate Interaction upon Metal Inclusion into a Porphyrin. *Chem. Eur. J.* **2012**, *18* (40), 12619-12623.
  39. Röckert, M.; Franke, M.; Tariq, Q.; Lungerich, D.; Jux, N.; Stark, M.; Kaftan, A.; Ditze, S.; Marbach, H.; Laurin, M.; Libuda, J.; Steinrück, H.-P.; Lytken, O., Insights in Reaction Mechanistics: Isotopic Exchange during the Metalation of Deuterated Tetraphenyl-21,23D-porphyrin on Cu(111). *J. Phys. Chem. C* **2014**, *118*, 26729-26736.
  40. Röckert, M.; Franke, M.; Tariq, Q.; Ditze, S.; Stark, M.; Uffinger, P.; Wechsler, D.; Singh, U.; Xiao, J.; Marbach, H.; Steinrück, H.-P.; Lytken, O., Coverage- and Temperature Dependent Metalation and Dehydrogenation of Tetraphenylporphyrin on Cu(111). *Chem. Eur. J.* **2014**, *20*, 8948-8953.
  41. Röckert, M.; Ditze, S.; Stark, M.; Xiao, J.; Steinrück, H.-P.; Marbach, H.; Lytken, O., Abrupt Coverage-Induced Enhancement of the Self-Metalation of Tetraphenylporphyrin with Cu(111). *J. Phys. Chem. C* **2014**, *118*, 1661-1667.
  42. Ruggieri, C.; Rangan, S.; Bartynski, R. A.; Galoppini, E., Zinc(II) Tetraphenylporphyrin on Ag(110) and Ag(111): Multilayer Desorption and Dehydrogenation. *J. Phys. Chem. C* **2016**, *120* (14), 7575-7585.
  43. Wiengarten, A.; Lloyd, J. A.; Seufert, K.; Reichert, J.; Auwärter, W.; Duncan, D. A.; Allegretti, F.; Fischer, S.; Oh, S. C.; Saglam, Ö.; Jiang, L.; Vijayaraghavan, S.; Écija, D.; Papageorgiou, A. C.; Barth, J. V., Cyclodehydrogenation; Break the Symmetry, Enhance the Selectivity. *Chem. Eur. J.* **2015**, *21*, 12285-12290.
  44. Albrecht, F.; Bischoff, F.; Auwärter, W.; Barth, J. V.; Repp, J., Direct Identification and Determination of Conformational Response in Adsorbed Individual Nonplanar Molecular Species Using Noncontact Atomic Force Microscopy. *Nano Lett.* **2016**, *16* (12), 7703-7709.
  45. Lepper, M.; Köbl, J.; Schmitt, T.; Gurrath, M.; Siervo, A. d.; Schneider, M. A.; Steinrück, H.-P.; Meyer, B.; Marbach, H.; Hieringer, W., "Inverted" porphyrins: a distorted adsorption geometry of free-base porphyrins on Cu(111). *Chem. Commun.* **2017**, *53*, 8207-8210.
  46. Stark, M.; Ditze, S.; Drost, M.; Buchner, F.; Steinrück, H. P.; Marbach, H., Coverage Dependent Disorder-Order Transition of 2H-Tetraphenylporphyrin on Cu(111). *Langmuir* **2013**, *29* (12), 4104-4110.